

Theoretical Study of the Excited States of Chlorin, Bacteriochlorin, Pheophytin *a*, and Chlorophyll *a* by the SAC/SAC–CI Method

J. Hasegawa, Y. Ozeki, K. Ohkawa, M. Hada, and H. Nakatsuji*[†]

Department of Synthetic and Biological Chemistry, Faculty of Engineering, Kyoto University, Sakyo-ku, Kyoto 606-01, Japan

Received: September 4, 1997; In Final Form: November 19, 1997

Excited states of free base chlorin (FBC), free base Bacteriochlorin (FBBC), pheophytin *a* (Pheo *a*), and chlorophyll *a* (Chlo *a*), which are derivatives of free base porphine (FBP), were calculated by the SAC (symmetry adapted cluster)/SAC–CI (configuration interaction) method. The results reproduced well the experimentally determined excitation energies. The reduction of the outer double bonds in the porphine ring in the order of FBP, FBC, and FBBC causes a breakdown of the symmetry and a narrowing of the HOMO–LUMO gap, which result in a red shift of the Q_x band and an increase of its intensity. In the change from Pheo *a* to Chlo *a*, the Mg coordination reduces the quasidegeneracy in the Q_x state and then increases the spectral intensity. The disappearance of the Q_y humps from the absorption spectrum of Pheo *a*, compared with that of Chlo *a*, is due to the red shift of the Q_y state.

Introduction

Many biological systems contain porphyrins, chlorins, and bacteriochlorins.^{1,2} These compounds often take an important part in biochemical reactions, such as light absorption, electron transfer,¹ and oxygen transport and storage.² Because of their scientific importance, they have been the subject of a wide variety of studies. In particular, the electronic structures of the ground and excited states of these compounds are an active field of interest.^{3–9} Semiempirical INDO/S calculations^{4,5} have been applied to elucidate the energetics of electron transfer in the photosynthetic reaction center. Using the ab initio method, some large-scale SCF calculations for the ground^{6,7} and anionized states⁷ have been reported. As for the excited states, although pioneering CI calculations⁸ have been reported for chlorophyllide *a* and pheophorbide *a*, there have been few calculations using a reliable ab initio method.

Porphyrin, chlorin, and bacteriochlorin have different π -electron conjugations. The number of reduced double bonds in the pyrrole rings is 0, 1, and 2 in porphyrins, chlorins, and bacteriochlorins, respectively. These reductions cause a considerable change in the excited states of these compounds, as seen in their absorption spectra.^{9,10} The simplest macrocycles without any substituents, i.e., free base porphine (FBP), free base chlorin (FBC), and free base bacteriochlorin (FBBC), are shown in Figure 1. From FBP to FBC, the absorption intensity of the first excited state, Q_x , increases.⁹ From FBC to FBBC, the Q_x absorption shows a red shift and increases further in its intensity, while the intense B (Soret) band shows a blue shift.¹⁰

Another characteristic of these macrocycles lies in their various substituents. Chlorophylls and bacteriochlorophylls have many substituents, e.g., an additional ring V and a long hydrocarbon chain (phytyl group). Simplified models of chlorophyll *a* (Chlo *a*) and pheophytin *a* (Pheo *a*) are shown in Figure 1, and they have only an additional ring V and the substituents that may affect the π -conjugations of the chlorin

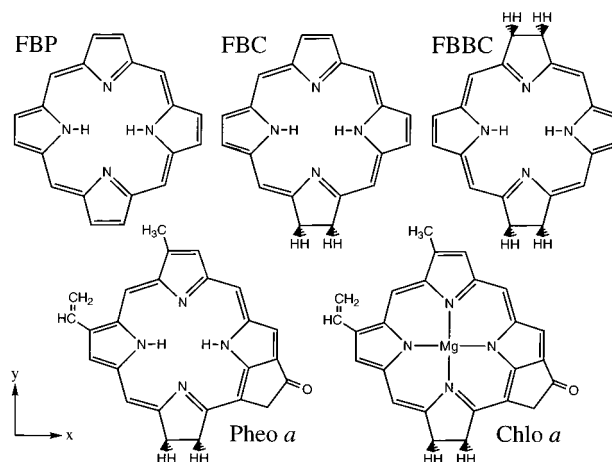


Figure 1. Molecular geometries of FBP, FBC, FBBC, Pheo *a*, and Chlo *a*. Some substituents in the X-ray structures of Pheo *a* and Chlo *a* are replaced by protons in the present calculations (see text).

ring. Another characteristic is metal coordination. Previous X-ray studies have revealed the entire structures of the photosynthetic reaction centers of some bacteria.^{1,11} They contain both Mg-coordinated bacteriochlorophylls and free base bacteriopheophytins. Spectroscopically, Mg coordination increases the absorption coefficient of the Q_x band.¹² This effect is interesting, since in a previous study on porphine and Mg-porphine,¹³ the Mg coordination affected only the symmetric degeneracy of the absorption and not the intensity of the Q_x band.

In this study, we examine the above features of the excited states of these macrocycles by the SAC¹⁴/SAC–CI¹⁵ method.¹⁶ The SAC/SAC–CI method has already been established as an efficient and reliable method for studying electron correlations in the ground and excited states of a variety of molecules and molecular systems¹⁶ including porphyrins.^{13,17–20} We study the excited-state electronic structures of FBP, FBC, and FBBC with regard to the differences in the π -conjugation. We then study the effects of the substituents and the Mg coordination on the

[†] Also belongs to The Institute for Fundamental Chemistry, 34-4 Takano Nishi-Hiraki-cho, Sakyo-ku, Kyoto 606, Japan.

TABLE 1: Dimensions of the SAC/SAC–CI Calculations for FBC, FBBC, Pheo *a*, and Chlo *a*

state	before selection	reference state	after selection ^a
FBC			
ground state (SAC)			
A ₁	7 009 800	1	22 810
excited states (SAC–CI)			
A ₁	7 009 800	4	70 206
B ₁	7 006 134	4	78 721
FBBC			
ground state (SAC)			
A _{1g}	3 661 607	1	28 190
excited states (SAC–CI)			
A _{1g}	3 661 607	1	26 672
B _{2u}	3 657 853	4	64 167
B _{3u}	3 657 832	4	71 162
Pheo <i>a</i>			
ground state (SAC)			
A	76 935 809	1	23 621
excited states (SAC–CI)			
A	76 935 809	4	60 692
Chlo <i>a</i>			
ground state (SAC)			
A	91 848 680	1	24 971
excited states (SAC–CI)			
A	91 848 680	4	71 422

^a Correlation energies for the ground states of FBC, FBBC, Pheo *a*, and Chlo *a* are -0.38933 , -0.48829 , -0.24554 , and -0.31067 hartree, respectively.

excited states of Pheo *a* and Chlo *a* in comparison with FBC. Conclusion of the study is given in the last section.

Computational Details

An optimized geometry²¹ is used for FBC. For FBBC, the same porphine skeleton as in FBP¹⁷ is used, except for the reduced pyrrole ring, for which the geometry used in a previous calculation⁹ was taken. FBC and FBBC are assumed to have C_{2v} and D_{2h} symmetries, respectively. For Pheo *a*, X-ray data²² are used, but for simplicity, some substituents are replaced by protons, except for the substituents that can conjugate with the π orbitals of the chlorin ring. For Chlo *a*, the Mg atom is coordinated to the central nitrogen atoms in Pheo *a*. These computational models are shown in Figure 1.

The basis sets used in this series of molecules are the same. Huzinaga's (63/5)/[2s2p] set²³ is used for C, N, and O atoms, and the (4)/[1s] set²⁴ is used for H. For Mg, we used Huzinaga's (533/5)/[5s/3p] set²³ plus two p-type polarization functions ($\zeta = 0.045$ and 0.143) and a d-type polarization function ($\zeta = 1.01$), which are the same as those used previously.¹³

In the SAC/SAC–CI calculations, only the inner-core orbitals are excluded from the active space. All single excitations and selected double excitations are included in the linked term. The energy threshold for the perturbation selection^{17,25} is 1×10^{-5} hartree for the ground state and for the excited state 5×10^{-7} and 1×10^{-6} hartree for π – π^* and other excitations, respectively. The results of the selections of the linked terms are shown in Table 1. The number of reference states is generally 4, so that the accuracy of the present calculations is not very good for the B states. The correlation energies calculated for the ground states of these compounds are also shown.

The Hartree–Fock SCF calculations are performed using the HONDO (ver. 8) program²⁶ and the SAC/SAC–CI calculations by the SAC85 program²⁷ modified for large-scale calculations.²⁸

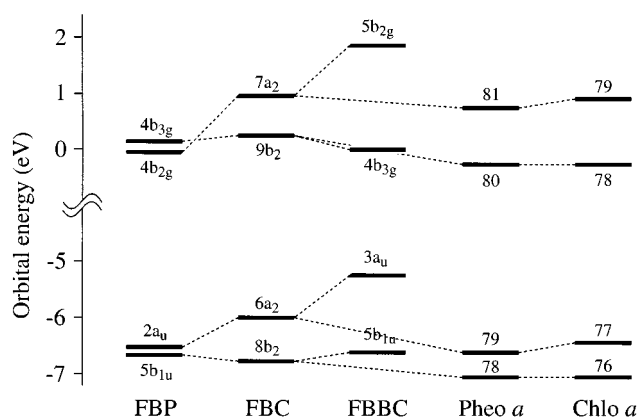


Figure 2. HF orbital energy levels of the “four orbitals” of FBP, FBC, FBBC, Pheo *a*, and Chlo *a*.

Excited States of FBP, FBC, and FBBC

FBP, FBC, and FBBC have π -conjugate systems that are different in the number of reduced pyrrole rings, as shown in Figure 1. The HF orbital energies of the HOMO, next-HOMO, LUMO, and next-LUMO of FBP, FBC, and FBBC are shown in Figure 2. Orbitals having similar characteristics are connected by dotted lines. As changing from FBP, FBC, to FBBC, the near degeneracies between the HOMO and next-HOMO and between the LUMO and next-LUMO, which are called the “four orbitals”,³ are removed considerably. It is already established that the “four orbitals” play crucial roles in the valence excited states of porphyrin compounds.^{3,13,17–20} Figure 2 shows that in FBP, FBC, and FBBC the reduction of the pyrrole rings considerably affects the energy levels of the HOMO, LUMO, and next-LUMO. The molecular orbital shapes of these “four orbitals” are shown in Figure 3. The next HOMOs of FBP, FBC, and FBBC have no amplitudes on the reduced pyrrole positions, so that their energy levels are scarcely changed, while the HOMOs have some coefficients so that the reduction destabilizes the MOs due to the shortening of the π -conjugation. Exactly the same argument is also valid for the LUMO and next-LUMO of these compounds.

The excited states of FBP, FBC, and FBBC as calculated by the SAC/SAC–CI method and the experimentally determined excitation energies are shown in Table 2. For FBBC, however, we could not find the experimental data, so that those of the bacteriochlorin derivative, bacteriopheophorbide (BPheo),¹⁰ are cited. The excitation energies calculated for FBP, FBC, and FBBC show good agreement with the experimental values, with an average discrepancy of 0.19 eV. The low-energy shift of the Q_x band from FBC to FBBC and the increase in the intensity of the Q_x band from FBP to FBBC are faithfully reproduced.

The first bands at 1.98 and 1.6 eV in FBC⁹ and BPheo¹⁰ are assigned to the x -polarized $1B_1$ and $1B_{3u}$ states, respectively, by comparison of the experimental values and the theoretical results. In FBC and FBBC, these Q_x states represent HOMO \rightarrow LUMO excitation which is strongly coupled with next-HOMO \rightarrow next-LUMO excitation. In FBP, the electronic structure of the Q_x state is characterized as quasidegenerate excited configurations. However, this quasidegeneracy is relaxed in FBC and FBBC, as shown in Table 2. The ratios of the weights of the two excitations are 1:0.70, 1:0.50, and 1:0.27 in FBP, FBC, and FBBC, respectively.

In FBC and FBBC, destabilization of the HOMO and next-LUMO levels produces red shifts and relaxation of the quasidegeneracy in the Q_x states. Table 3 shows the energies and the orbital energy gaps for the main configurations of the Q_x bands.

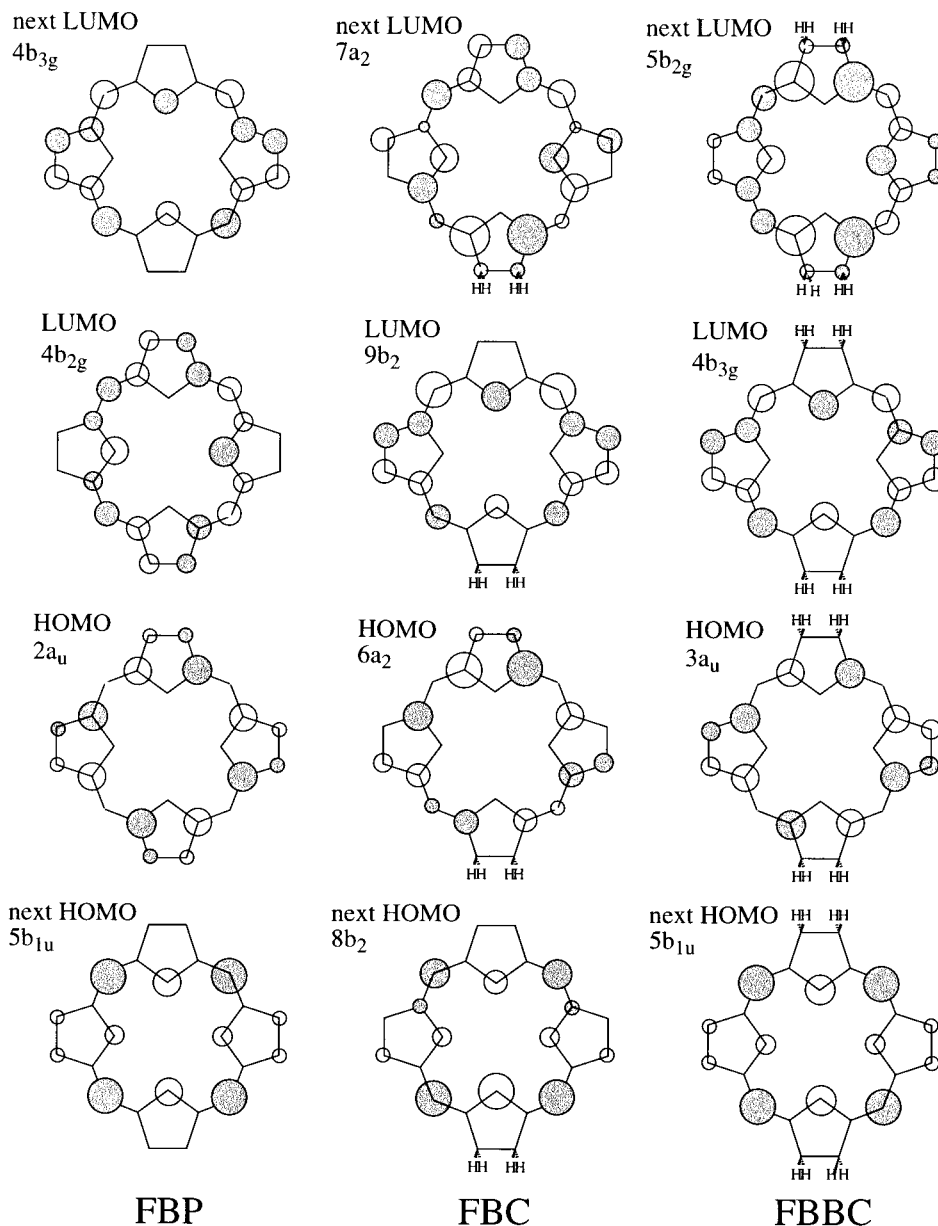


Figure 3. Illustration of the "four orbitals" of FBP, FBC, and FBBC.

In FBP, the energies of the $5b_{1u} \rightarrow 4b_{2g}$ and $2a_u \rightarrow 4b_{3g}$ excited configurations are similar: 4.15 and 4.22 eV, respectively. However, in FBC and FBBC, destabilization of the HOMO and next-LUMO levels makes the orbital energy gap ($\Delta\epsilon$ in Table 3) between the HOMO and LUMO small and that between the next-HOMO and next-LUMO large. The energies of the HOMO \rightarrow LUMO configurations are stabilized and those of the next-HOMO \rightarrow next-LUMO configurations are destabilized in FBC and FBBC, as shown in Table 3. Since a greater energy difference leads to a weaker coupling of the two configurations, the Q_x state takes a greater HOMO \rightarrow LUMO character and a smaller excitation energy. The main factor of these energy shifts of the configurations is the change of the orbital energy gaps, $\Delta\epsilon$, as shown in Table 3. The Coulomb and exchange integrals that appear in the diagonal term have little contribution to these energy changes.

The relaxation of the quasidegeneracy leads to an increase in the intensity of the Q_x bands in FBC and FBBC. In FBP, the two main configurations are almost degenerate, and the transition moments of each configuration cancel each other. The contributions of the $5b_{1u} \rightarrow 4b_{2g}$ and $2a_u \rightarrow 4b_{3g}$ excited

configurations to the transition moment (product of the SAC-CI coefficient and the transition dipole moment for each configuration) are -3.18 and 2.85 , respectively, which offset each other. This causes the small intensity of the FBP Q_x band.^{19,34} However, the quasidegeneracy in FBP is relaxed in FBC and FBBC. The difference in the SAC-CI coefficients causes incomplete cancellation of the transition moment and an increase in the intensity of the Q_x band in FBC and FBBC. Weiss³⁴ identified this incomplete cancellation mechanism using a qualitative model. The present results support this mechanism.

Further, the change in the configuration-transition dipole moment due to the HOMO \rightarrow LUMO excitation itself, $\langle 0|r|HOMO \rightarrow LUMO \rangle$ ($r = x, y, z$), is also a cause of the increase in the transition dipole of the Q_x states in FBBC. The configuration-transition dipole moment is shown in Table 3. The value of the element in FBBC, $\langle 0|x|3a_u \rightarrow 4b_{3g} \rangle$, (5.60) is larger than that in FBP, $\langle 0|x|5b_{1u} \rightarrow 4b_{2g} \rangle$, (4.61) or FBC, $\langle 0|x|6a_2 \rightarrow 9b_2 \rangle$ (4.60). To better understand which atoms have a large contribution, a population analysis for the transition dipole moment in the HOMO \rightarrow LUMO configuration for FBC and FBBC and in the HOMO \rightarrow next-LUMO configuration for

TABLE 2: Excited States of FBP, FBC, FBBC, Pheo *a*, and Chlo *a* Calculated by the SAC/SAC–CI Method

state	SAC–CI			exptl	
	main configuration ($C \geq 0.2 $)	nature	excitation energy (eV)	oscillator strength	excitation energy (eV)
FBP^a					
1B _{3u}	0.73(5b _{1u} →4b _{2g})+0.61(2a _u →4b _{3g})	π - π^*	1.75	1.13×10^{-3} ; x	1.98 ^b , 2.02 ^c ; Q _x
1B _{2u}	-0.70(2a _u →4b _{2g})-0.66(5b _{1u} →4b _{3g})	π - π^*	2.23	5.66×10^{-3} ; y	2.42 ^b , 2.39 ^c ; Q _y
2B _{3u}	-0.64(2a _u →4b _{3g})+0.52(4b _{1u} →4b _{2g})-0.43(5b _{1u} →4b _{2g})	π - π^*	3.59	1.03; x	3.33 ^b , 3.15 ^c ; B
2B _{2u}	0.66(5b _{1u} →4b _{3g})-0.63(2a _u →4b _{2g})-0.25(4b _{1u} →4b _{3g})	π - π^*	3.79	1.73; y	3.65 ^b ; N
FBC					
1B ₁	-0.78(6a ₂ →9b ₂)-0.55(8b ₂ →7a ₂)	π - π^*	1.68	6.24×10^{-2} ; x	1.98 ^c , 1.94 ^d ; Q _x
2A ₁	-0.75(8b ₂ →9b ₂)+0.58(6a ₂ →7a ₂)	π - π^*	2.39	8.02×10^{-3} ; y	2.29 ^c , 2.29 ^d ; Q _y
2B ₁	-0.75(8b ₂ →7a ₂)+0.53(6a ₂ →9b ₂)-0.22(7b ₂ →7a ₂)	π - π^*	3.58	1.28; x	3.18 ^c , 3.19 ^d ; B
3A ₁	0.72(6a ₂ →7a ₂)+0.56(8b ₂ →9b ₂)+0.22(7b ₂ →9b ₂)	π - π^*	3.74	1.68; y	
FBBC					
1B _{3u}	0.85(3a _u →4b _{3g})+0.44(5b _{1u} →5b _{2g})	π - π^*	1.47	1.88×10^{-1} ; x	(1.6) ^e ; Q _x
1B _{2u}	0.77(5b _{1u} →4b _{3g})-0.54(3a _u →5b _{2g})	π - π^*	2.42	2.57×10^{-2} ; y	(2.3) ^e ; Q _y
2B _{2u}	-0.77(3a _u →5b _{2g})-0.54(5b _{1u} →4b _{3g})-0.20(4b _{1u} →4b _{3g})	π - π^*	4.11	1.86; y	(3.1[shoulder]) ^e ; B
2B _{3u}	-0.84(5b _{1u} →5b _{2g})+0.44(3a _u →4b _{3g})	π - π^*	4.24	2.11; x	(3.4) ^e ; B
Pheo <i>a</i>					
2A	-0.74(79→80)-0.51(78→81)-0.23(79→81)	π - π^*	1.81	7.22×10^{-2} ; x	1.9 ^f , 1.86 ^g , 1.87 ^d ; Q _x
3A	-0.74(78→80)+0.52(79→81)-0.28(79→80)	π - π^*	2.33	4.57×10^{-2} ; y	2.3 ^f , 2.33 ^g , 2.30 ^d ; Q _y
4A	-0.73(78→81)+0.51(79→80)	π - π^*	3.37	1.20; x	3.1 ^f , 3.04 ^g ; B
5A	-0.72(79→81)-0.50(78→80)+0.24(78→81)+0.22(77→80)	π - π^*	3.52	1.03; y	3.2 ^f ; B
Chlo <i>a</i>					
2A	0.81(77→78)-0.37(76→79)-0.25(76→78)+0.21(77→79)	π - π^*	1.81	0.179; x	1.87 ^h , 1.88 ^g ; Q _x
3A	-0.77(76→78)+0.44(77→79)-0.31(77→78)	π - π^*	2.17	8.26×10^{-2} ; y	2.14 ^h , 2.16 ^g ; Q _y
4A	+0.78(77→79)+0.42(76→78)+0.26(74→78)	π - π^*	3.48	1.01; y	2.88 ^h , 2.90 ^g ; B
5A	-0.84(76→79)+0.35(77→78)	π - π^*	3.65	1.38; x	

^a Reference 17. ^b In gas phase. Reference 29. ^c In benzene. Reference 9. ^d In benzene. Reference 30. ^e Data for bacteriopheophorbide and not for FBBC. Reference 10. ^f Reference 10. ^g In ether. Reference 32. ^h In ether. Reference 33.

TABLE 3: Energies (in eV) and Moments (in au) of the Main Configurations of the Q_x Band for FBP, FBC, FBBC, Pheo *a*, and Chlo *a*

	FBP		FBC		FBBC	
	5b _{1u} →4b _{2g}	2a _u →4b _{3g}	6a ₂ →9b ₂	8b ₂ →7a ₂	3a _u →4b _{3g}	5b _{1u} →5b _{2g}
weight	0.53	0.37	0.61	0.30	0.72	0.19
$\langle 0 x i \rightarrow a \rangle^a$	4.61	-4.67	4.60	-3.41	5.60	-3.92
Δe^b	6.62	6.66	6.28	7.72	5.24	8.46
energy ^c	4.15	4.22	3.71	4.71	3.27	5.37
	Pheo <i>a</i>			Chlo <i>a</i>		
	79→80	78→81	78→80	77→78	76→79	76→78
weight	0.56	0.26	0.04	0.66	0.14	0.06
$\langle 0 x i \rightarrow a \rangle^a$	4.41	-3.24	-0.13	4.51	3.08	-0.93
$\langle 0 y i \rightarrow a \rangle^a$	1.58	-1.47	3.39	1.22	1.03	3.61
Δe^b	6.35	7.77	6.82	6.18	7.99	6.81
energy ^c	3.87	4.91	4.23	3.68	5.09	4.23

^a Transition moments of the configurations. ^b Orbital energy gap in eV. ^c Energy of the main configuration relative to that of the HF configuration.

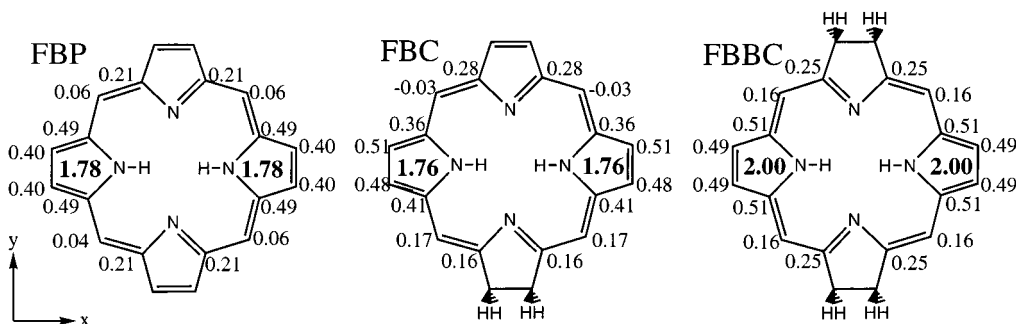


Figure 4. Population analysis for the transition moment of the HOMO → LUMO excitation configuration of FBC and FBBC and the HOMO → next-LUMO excitation configuration of FBP. Atoms with contributions larger than 0.01 are shown.

FBP were calculated as in a Mulliken population analysis, as explained in the Appendix. Figure 4 shows the results of the

analysis for the atoms whose contributions are greater than 0.01. The sum of the atomic transition moments of the pyrrole rings

having N–H bonds increases considerably in FBBC. This finding is related to the π -conjugation narrowing caused by the reduction of the pyrrole rings in FBBC.

The second bands at 2.29 and 2.3 eV in FBC⁹ and BPho¹⁰ are assigned to the y -polarized $2A_1$ and $1B_{2u}$ states calculated at 2.39 and 2.42 eV, respectively. This assignment agrees with the conventional one,^{9,31} and the ordering of the polarization directions of the Q bands is the same as in FBP. The Q_y bands of FBC and FBBC are characterized as the next-HOMO \rightarrow LUMO excitation, which is strongly coupled with the HOMO \rightarrow next-LUMO excitation. The effects of the reduction on the excitation energy and the configuration mixing of the Q_y bands are small, as shown in Table 2, since the energy gaps between next-HOMO and LUMO and between HOMO and next-LUMO are affected very little, as seen in Figure 2, by the reduction from FBP to FBC and to FBBC.

As for the B band in FBC, the strong peak at 3.18 eV in the absorption spectrum⁹ is assigned to the x -polarized $2B_1$ state calculated at 3.59 eV. Our SAC–CI SD-R calculation tends to overestimate the excitation energy of the B band.¹⁶ This state is characterized as next-HOMO \rightarrow next-LUMO excitation, which is strongly coupled to HOMO \rightarrow LUMO excitation. The broad shoulder⁹ on the blue side is assigned to the y -polarized $3A_1$ state calculated at 3.74 eV, which is characterized as HOMO \rightarrow next-LUMO excitation coupled to next-HOMO \rightarrow LUMO excitation. The order of polarization is supported by experimental results.³⁵ Previous MRSD π CI calculations by Nagashima et al.⁹ gave the same assignment. As for FBBC, the calculation indicates that the $2B_{2u}$ (B_y) and $2B_{3u}$ (B_x) states are at 4.11 and 4.24 eV, respectively, which may overestimate the experimental values. Their characters are HOMO \rightarrow next-LUMO excitation and next-HOMO \rightarrow next-LUMO excitation, respectively. The B states of FBBC shift to a higher energy region than those of FBP and FBC. Since we cannot find experimental data for the B band of FBBC, direct comparison with experiments is impossible. However, the same blue shifts were observed in the absorption spectra of their derivatives, bacteriopheophorbide and pheophorbide.¹⁰

In FBBC, the ordering of the B_x and B_y states are reversed due to the high-energy shift of the B_x state in FBBC. With respect to the orbital energy difference, the B_x state is higher than the B_y state in FBP, FBC, and FBBC, as seen from Figure 2. However, after SAC–CI treatment, the B_x state is more stable than the B_y state in FBP and FBC. This is very general as seen in our previous studies on porphyrins.^{16,19} In FBBC, since the energy difference between the two configurations is very large, the coupling between the two main configurations is weakened and then the B_x state lies on the blue side of the B_y state. Experimental examination of the order of the polarizations of the peaks involved in the B band is very interesting.

Excited States of Pheo *a* and Chlo *a*

In the photosynthetic reaction center of plants, chlorophyll and pheophytin play important roles in the electron transfer. Chlorophyll is a substituted and Mg-coordinated chlorin, and pheophytin¹⁰ is a free base form of chlorophyll. The absorption spectrum of pheophytin is almost the same as that of FBC with regard to the excitation energy,^{10,30} although the vinyl group and ring V seem to affect the π -electron system of the chlorin ring through π -conjugation, since in X-ray coordinates the molecular plane of these substituents is parallel to that of the chlorin ring.²² On the other hand, with Mg coordination, the absorption spectrum of chlorophyll^{10,32} is much different from that of pheophytin.³² First, the intensity of the first excited state

increases. Second, the double humps in the 500-nm region of pheophytin spectrum are not found in the chlorophyll one. This coordination effect is very interesting, since for FBP, the Mg coordination only affects the symmetric degeneracy in the absorption spectrum.¹³

Substitutions and Mg coordination affect orbital energy. The HF orbital energy levels of the “four orbitals” for Pheo *a* and Chlo *a* are also shown in Figure 2. In comparing FBC and Pheo *a*, the substitution stabilizes the HOMO (79th MO) and the LUMO (80th MO). Actually, small orbital mixing of the substituent orbitals (the vinyl group and oxygen in ring V) is observed in the HOMO and LUMO of Pheo *a*. In comparing Pheo *a* and Chlo *a*, the Mg coordination slightly destabilizes the orbital energy of the HOMO (77th MO) and next-LUMO (79th MO) by 0.1 and 0.2 eV, respectively, while those of the LUMO and next-HOMO are almost unchanged. Little, if any, orbital mixing between Mg and the “four orbitals” is seen in Chlo *a*.

The calculated excited states of Pheo *a* and Chlo *a* are shown in Table 2. As for the Q band, the SAC–CI results reproduce well the experimental peak positions and the increase in the intensity of the first excited state in Chlo *a*. As for the B band, the present results overestimate the experimental excitation energies.

The first bands of Pheo *a* and Chlo *a*, which are the Q_x bands both at 1.87 eV,^{32,33} are assigned to the x -polarized $2A$ excited state, both calculated at 1.81 eV. In comparison with the Q_x band of FBC observed at 1.98 eV and calculated at 1.68 eV, the substituents and the Mg coordination do not have a large effect on the excitation energy of the Q_x state. However, as shown in Table 3, the energies of the configurations that comprise the Q_x states of these compounds are different. For Pheo *a*, the two main configurations shift equally to a higher energy region by about 0.2 eV, compared to FBC. For Chlo *a*, the HOMO \rightarrow LUMO excitation is stabilized by 0.19 eV and the next-HOMO \rightarrow next-LUMO excitation is destabilized by 0.18 eV, compared to Pheo *a*. For Pheo *a*, the ratio of the weights of the two configurations is the same as in FBC, due to the parallel energy shifts of the two main configurations. However, in Chlo *a*, the weight of the HOMO \rightarrow LUMO excitation increases and that of the next-HOMO \rightarrow next-LUMO excitation decreases. The configuration interactions give a different mixing of the configurations but accidentally similar excitation energies.

The difference in the configuration mixing leads to different properties of the Q_x states of Pheo *a* and Chlo *a*, i.e., the transition moment. In comparing FBC and Pheo *a*, the spectral intensities of the Q_x bands are similarly small, since in each molecule, the contributions to the transition moments due to the two main configurations cancel each other owing to the similarity of the SAC–CI coefficient.¹⁹ On the other hand, Chlo *a* shows different configuration mixing, as mentioned above, so that the cancellation is rather incomplete, leading to a greater intensity of Chlo *a* than that of FBC and Pheo *a*.

For FBP, FBC, and FBBC, the incomplete cancellation is caused by the coefficients and the transition moments of the configurations, as examined in section 3. For FBC, Pheo *a*, and Chlo *a*, the transition moments of the configurations are similar, as shown in Table 3, because of a small mixing with the substituents and Mg. Therefore, the incomplete cancellation in Pheo *a* and Chlo *a* is mainly due to the breakdown of the quasidegeneracy.

In our previous study on Mg–porphine (MgP),¹³ Mg coordination was shown to have little effect on the intensity of the

Q band. In the Q state of MgP, the two main configurations were almost degenerate. Due to the Mg coordination in FBP, the weight of the most important configuration, $5b_{1u} \rightarrow 4b_{2g}$, decreased due to a destabilization of the $4b_{2g}$ orbital, while that of the next most important configuration, $2a_u \rightarrow 4b_{3g}$, increased due to a destabilization of the $2a_u$ orbital, which leads to a more degenerate situation. Therefore, the cancellation of the transition moments between these two excitations was almost complete in MgP. However, in Chlo *a*, a destabilization of the HOMO (77th MO) contributes to an increase in the weight of the most important HOMO \rightarrow LUMO excitation and a destabilization of the next LUMO (79th MO) contributes to the decrease in the weight of the next most important $76 \rightarrow 79$ excitation. This causes a reduction in the quasidegeneracy of the two main configurations and give a net transition moment due to an incomplete cancellation of the two contributions.

The second bands measured at 2.3 eV for Pheo *a*^{10,30,32} and at 2.1 eV for Chlo *a*^{32,33} were assigned to the *y*-polarized 3A excited states calculated at 2.33 and 2.17 eV, respectively. The disappearance of the humps at 480–550 nm in the Pheo *a* spectrum^{10,30,32} is explained by the red shift of the 3A state in Chlo *a*. The main configurations of the 3A states of Pheo *a* and Chlo *a* consist of the next-HOMO \rightarrow LUMO excitation strongly coupled to the HOMO \rightarrow next-LUMO excitation.

As for the B band, the SAC–CI calculations reproduce the experimental absorption of Pheo *a* with a discrepancy of 0.28 eV, but overestimate that of Chlo *a* by 0.6 eV. As for Pheo *a*, the strong peak and the shoulder of the B band are assigned to the *x*-polarized 4A state and the *y*-polarized 5A state, calculated at 3.37 and 3.52 eV, respectively. These states are characterized as next-HOMO \rightarrow next-LUMO excitation and HOMO \rightarrow LUMO excitation, respectively. The ordering of the polarizations of the B band of Pheo *a* is the same as that of FBC. In a previous fluorescence polarization study in *meso*-pyromethyl pheophorbide, the ordering of the polarization was considered to be lower *y*-polarization and higher *x*-polarization, and the substituents were thought to change the order of the polarizations.³⁶ However, a more recent fluorescence polarization study on pheophorbide *a* by Goedheer³³ showed a different result in that the lower and higher sides of the B band are *x*- and *y*-polarizations, respectively. Our SAC–CI results support Goedheer's results. In our study, the substituents did not change the order of the polarizations.

The peak of the B band of Chlo *a* is observed at 2.90 eV in ether.³⁵ The SAC–CI calculation gives an excitation energy of 3.48 eV (*y*-polarizations). The counterpart of the B state is calculated at 3.65 eV (*x*-polarizations). This ordering is different from that of Pheo *a* and FBC, but corresponds to the experimental results.^{32,33,36–38} The Mg coordination reverses the order of the polarization in the B band of Chlo *a* from that of Pheo *a*.

In the SECI calculations of FBC and Pheo *a*, the polarizations of the B states were *y*- and *x*-polarization in the order of increasing energy, in contrast to the results of the SAC–CI calculation. In FBC and Pheo *a*, the *x*-polarized B states which are dominated by next-HOMO \rightarrow next-LUMO excitation are stabilized by strong mixing with low-energy HOMO \rightarrow LUMO excitation. By the SAC–CI treatment, the weights of the HOMO \rightarrow LUMO excitations in the B_x states are further increased in FBC and Pheo *a*. This causes the *x*-polarized B states to be more stable than the *y*-polarized B states. However, in Chlo *a*, the SAC–CI treatment increases the weight of the next-HOMO \rightarrow next-LUMO excitation in the *x*-polarized B

states. These results show the importance of the electron correlations for the descriptions of the B states.

Conclusion

The excited states of biochemically important compounds FBC, FBBC, Pheo *a*, and Chlo *a* were calculated by the SAC/SAC–CI method. The results of calculations well reproduced the absorption spectra of these compounds. This together with the previous results for porphyrins^{13,17–20} shows that the SAC/SAC–CI method, which gives accurate results for small molecules,¹⁶ is also applicable to relatively large biochemical compounds. These results encourage us to apply the SAC–CI method to the energetics of biochemical reactions, including different electronic excited states.

The effects of the reduction in the pyrrole rings of the porphyrins are studied for the absorption spectra of FBP, FBC, and FBBC. Such reduction destabilized the HOMO and next-LUMO levels due to a shortening in the π -conjugation of these compounds. Since the HOMO–LUMO gap decreases, the Q_x states shift to a lower energy region and their quasidegenerate characteristics are relaxed, causing an incomplete cancellation in the transition dipole moment, which leads to an increase in the intensity of the Q_x band of FBBC relative to that of FBP. Further, an increase in the configuration-transition dipole moment itself is also a reason for the increase of the transition intensity.

The effects of the substitutions and the Mg coordination were analyzed. The substitutions do not affect the HOMO–LUMO gap of Pheo *a*. On the other hand, in Chlo *a*, the Mg coordination reduced the HOMO–LUMO gap, causing a breakdown of the quasidegenerate character of the Q_x state. This leads to an increase of the intensity of the Q_x band of Chlo *a* due to a smaller cancellation of the transition moment than in Pheo *a*.

Acknowledgment. This study was supported in part by a Grant-in-Aid for Scientific Research from the Japanese Ministry of Education, Science, Culture, and Sports, and by the New Energy and Industrial Technology Development Organization (NEDO). One of the authors (J.H.) gratefully acknowledges the Research Fellowships from the Japan Society for the Promotion of Science for Young Scientists.

Appendix

Molecular orbitals φ_i are described in the LCAO approximation as

$$\varphi_i = \sum_r C_{ir} \chi_r \quad (1)$$

where χ_r is an atomic orbital and C_{ir} a MO coefficient. The transition dipole matrix element for a single excitation is written as

$$\begin{aligned} \langle \Phi_{\text{HF}} | Q | \Phi_{i \rightarrow a} \rangle &= \sqrt{2} \langle \varphi_i | Q | \varphi_a \rangle \\ &= \sqrt{2} \sum_{r,s} C_{ri} C_{sa} \langle \chi_r | Q | \chi_s \rangle \end{aligned} \quad (2)$$

where *i* and *a* show occupied and unoccupied orbitals, respectively, and Φ_{HF} denotes the HF configuration. *Q* is a dipole operator (*Q* = *x*, *y*, or *z*). Equation 2 can be divided into the contribution of each atom:

$$\langle \Phi_{\text{HF}} | Q | \Phi_{i \rightarrow a} \rangle = \sum_A \langle Q \rangle_A \quad (3)$$

where the atomic contribution to the transition dipole element is written as

$$\langle Q \rangle_A = \sqrt{2} \sum_{r \in \text{AtomA}} \sum_s C_{ri} C_{sa} \langle \chi_r | Q | \chi_s \rangle \quad (4)$$

like the Mulliken population analysis.

References and Notes

- (1) Michel-Beyerle, M. E. In *Antennas and Reaction Centers of Photosynthetic Bacteria*; Springer-Verlag: Berlin, 1985.
- (2) Scheidt, W. D.; Reed, C. A. *Chem. Rev. (Washington, D.C.)* **1981**, *81*, 543.
- (3) Gouterman, M. In *The Porphyrin*; Dolphin, D., Ed.; Academic Press: New York, 1978; Vol III.
- (4) Thompson, M. A.; Zerner, M. C. *J. Am. Chem. Soc.* **1991**, *113*, 8210.
- (5) Scherer, P. O. J.; Scharnagl, C.; Fischer, S. F. *Chem. Phys.* **1995**, *197*, 333.
- (6) Zhang, L. Y.; Friesner, R. A. *J. Phys. Chem.* **1995**, *99*, 16479.
- (7) Sakuma, T.; Kashiwagi, T.; Takada, H.; Nakamura, H. *Int. J. Quantum Chem.* **1997**, *61*, 137.
- (8) Christoffersen, R. E. *Int. J. Quantum Chem.* **1979**, *16*, 573.
- (9) Nagashima, U.; Takada, T.; Ohno, K. *J. Chem. Phys.* **1986**, *85*, 4524.
- (10) Scheer, H.; Inhoffen, H. H. In *The Porphyrin*; Dolphin, D., Ed.; Academic Press: New York, 1978; Vol II, pp 45–90.
- (11) Desienhofer, J.; Epp, O.; Miki, K.; Huber, R.; Michel, H. *J. Mol. Biol.* **1984**, *180*, 385.
- (12) Weiss, C. *J. Mol. Spectrosc.* **1972**, *44*, 37.
- (13) Hasegawa, J.; Hada, M.; Nonoguchi, M.; Nakatsuji, H. *Chem. Phys. Lett.* **1996**, *250*, 159.
- (14) Nakatsuji, H.; Hirao, K. *J. Chem. Phys.* **1978**, *68*, 2035.
- (15) Nakatsuji, H. *Chem. Phys. Lett.* **1978**, *59*, 362; **1979**, *67*, 329, 334.
- (16) Nakatsuji, H. In *Computational Chemistry*; Leszczynski J., Ed.; World Scientific: Singapore, 1997; Vol II, pp 62–124. Nakatsuji, H. *Acta Chim. Hung.* **1992**, *129*, 719.
- (17) Nakatsuji, H.; Hasegawa, J.; Hada, M. *J. Chem. Phys.* **1996**, *104*, 2321.
- (18) Nakatsuji, H.; Hasegawa, J.; Ueda, H.; Hada, M. *Chem. Phys. Lett.* **1996**, *250*, 379.
- (19) Toyota, K.; Hasegawa, J.; Nakatsuji, H. *Chem. Phys. Lett.* **1996**, *250*, 437.
- (20) Nakatsuji, H.; Tokita, Y.; Hasegawa, J.; Hada, M. *Chem. Phys. Lett.* **1996**, *256*, 220. Tokita Y.; Nakatsuji, H. *J. Phys. Chem. B* **1997**, *101*, 3281.
- (21) Almlöf, J.; Fisher, T. H.; Gassman, P. G.; Ghosh, A.; Häser, M. *J. Phys. Chem.* **1993**, *97*, 10964.
- (22) Fisher, M. S.; Templeton, D. H.; Zalkin, A.; Calvin, M. *J. Am. Chem. Soc.* **1982**, *104*, 3613.
- (23) Huzinaga, S.; Andzelm, J.; Klobukowski, M.; Radzio-Andzelm, E.; Sakai, Y.; Tatewaki, H. In *Gaussian Basis Set for Molecular Calculations*; Elsevier: New York, 1984.
- (24) Huzinaga, S. *J. Chem. Phys.* **1965**, *42*, 1293.
- (25) Nakatsuji, H. *Chem. Phys.* **1983**, *75*, 425.
- (26) Dupuis, M.; Farazdel, A. *MOTECC-91*; Center for Scientific and Engineering Computations, IBM Corp. 1991.
- (27) Nakatsuji, H. *Program System for SAC and SAC-CI Calculations*, Program Library No. 146 (Y4/SAC), Data Processing Center of Kyoto University, 1985. Program Library SAC85, No. 1396, Computer Center of the Institute for Molecular Science, Okazaki, 1981.
- (28) Nakatsuji, H.; Hada, M.; Ehara, M.; Hasegawa, J.; Nakajima, T.; Nakai, H.; Kitao, O.; Toyota, K. SAC/SAC-CI Program System (SAC-CI96) for Calculating Ground, Excited, Ionized, and Electron Attached States and Singlet to Septet Spin Multiplicities, to be submitted.
- (29) Edwards, L.; Dolphin, D. H. *J. Mol. Spectrosc.* **1971**, *38*, 16.
- (30) Eisner, U.; Linstead, R. P. *J. Chem. Soc.* **1955**, 3742.
- (31) Seely, G. R. *J. Chem. Phys.* **1957**, *27*, 125.
- (32) Houssier, C.; Sauer, K. *J. Am. Chem. Soc.* **1970**, *92*, 779.
- (33) Goedheer, J. C. In *The Chlorophylls*; Vernon, L., Seely, G. R., Eds.; Academic Press: New York, 1966.
- (34) Weiss, C. In *The Porphyrin*; Dolphin, D., Ed.; Academic Press: New York, 1978; Vol III.
- (35) Sevchenko, A. N.; Solov'ev, K. N.; Mashenkov, V. A.; Shkirman, S. F. Losev, A. P. *Sov. Phys.-Dokl.* **1966**, *10*, 778.
- (36) Bär, F.; Lang, H.; Schnabel, E.; Kurn, H. *Z. Electrochim.* **1961**, *65*, 346.
- (37) Gouterman, M.; Stryer, L. *J. Chem. Phys.* **1962**, *37*, 2260.
- (38) Houssier, C.; Sauer, K. *Biochim. Biophys. Acta* **1969**, *172*, 492.